CHEMICAL PHYSICS

Collisions of ultracold $^{23}Na^{87}Rb$ molecules with controlled chemical reactivities

Xin Ye,[1] Mingyang Guo,[1] Maykel L. González-Martínez,[2] Goulven Quéméner,[2] Dajun Wang[1,3]*

Copyright © 2018 The Authors, some rights reserved; exclusive licensee American Association for the Advancement of Science. No claim to original U.S. Government Works. Distributed under a Creative Commons Attribution NonCommercial License 4.0 (CC BY-NC).

The collision of molecules at ultracold temperatures is of great importance to understand the chemical interactions at the quantum regime. Although much theoretical work has been devoted to this, experimental data are only sparsely available, mainly because of the difficulty in producing ground-state molecules at ultracold temperatures. We report here the creation of optically trapped samples of ground-state bosonic sodium-rubidium molecules with precisely controlled internal states and, enabled by this, a detailed study on the inelastic loss with and without the NaRb + NaRb → Na_2 + Rb_2 chemical reaction. Contrary to intuitive expectations, we observed very similar loss and heating, regardless of the chemical reactivities. In addition, as evidenced by the reducing loss rate constants with increasing temperatures, we found that these collisions are already outside the Wigner region although the sample temperatures are sub-microkelvin. Our measurement agrees semiquantitatively with models based on long-range interactions but calls for a deeper understanding on the short-range physics for a more complete interpretation.

INTRODUCTION

Collisional study is a primary way to understand the interaction between particles; for example, much of today's knowledge on chemical reaction dynamics can be attributed to pioneering studies on elementary reaction processes with crossed molecular beam experiments (*1*). In recent years, owing to the development of ultracold technologies, controlling the external motion between particles to the unprecedented single and lowest relative angular momentum level has become routinely available. In this quantum regime, theoretical studies have suggested early on that chemical reactions can happen efficiently with the help of quantum effects such as tunneling (*2*). In 2010, this ultracold chemical reaction was first confirmed via measuring the loss in a gaseous sample of chemical-reactive $^{40}K^{87}Rb$ molecules (*3*).

Besides its relevance in ultracold chemistry, understanding the basic molecular interaction at ultralow collision energies is also a necessary step toward unveiling the full potential of ultracold polar molecules (UPMs) on a very broad range of applications in quantum simulation of exotic many-body physics (*4*, *5*), quantum information (*6*, *7*), and precision measurements for fundamental constants. In several recently created UPMs, including fermionic $^{23}Na^{40}K$ (*8*) and bosonic $^{87}Rb^{133}Cs$ (*9*, *10*) and $^{23}Na^{87}Rb$ (*11*), which are all nonreactive and thus thought to be immune to inelastic collisions, large losses were still observed. Presently, this unexpected loss has become a major obstacle for advancing the field because it prohibits the quest for quantum-degenerate UPMs via evaporative cooling. Although there is still no definitive explanation for this loss, it is generally believed that the four-atom collision complex formed following the encounter of two molecules plays a key role (*12*).

Here, we present a direct comparison on the inelastic losses of UPMs with and without the bimolecular chemical reaction energetically allowed. This study is performed with optically trapped ultracold gases of bosonic $^{23}Na^{87}Rb$ molecules with their chemical reactivity controlled via vibrational state manipulation (hereafter, ^{23}Na and ^{87}Rb will be denoted as Na and Rb, respectively). Vibrational excitation has already been established as an efficient way to control both the chemical reaction rate and the outcome since the 1970s (*13*–*16*), but it has never been exploited in ultracold molecular samples.

[1]Department of Physics, The Chinese University of Hong Kong, Hong Kong SAR, China. [2]Laboratoire Aimé Cotton, CNRS, Université Paris-Sud, ENS Paris-Saclay, Université Paris-Saclay, 91405 Orsay Cedex, France. [3]Shenzhen Research Institute, The Chinese University of Hong Kong, Shenzhen, China.
*Corresponding author. Email: djwang@cuhk.edu.hk

The main feature of the Na and Rb diatomic molecules that enables our investigation is illustrated schematically in Fig. 1. For NaRb molecules in the absolute ground state, the reaction

$$\mathrm{NaRb}(v=0,J=0)+\mathrm{NaRb}(v=0,J=0)\rightarrow \mathrm{Na_2}(v=0,J=0)+\mathrm{Rb_2}(v=0,J=0) \quad (1)$$

is endothermic by 47 cm^{-1} (*17*–*20*). Here, v and J are the vibrational and rotational quantum numbers, respectively. The situation is starkly different for NaRb in the first excited vibrational level because the reaction

$$\mathrm{NaRb}(v=1,J=0)+\mathrm{NaRb}(v=1,J=0)\rightarrow \mathrm{Na_2}(v=0,J=0)+\mathrm{Rb_2}(v=0,J=0) \quad (2)$$

is exothermic by 164 cm^{-1} (*17*–*20*). Actually, when two (v = 1, J = 0) NaRb molecules react, this large amount of energy released can be disposed into many vibrational and rotation levels of the Na_2 and Rb_2 product molecules as well as the relative translational motions (partial waves) between them. This reaction, as well as all other bimolecular reactions between alkali molecules (*17*, *21*), should be barrierless with the Na_2Rb_2 potential well lying thousands of wave numbers below both the NaRb + NaRb and the Na_2 + Rb_2 asymptotic limits.

The long-range bimolecular NaRb interaction coefficient for (v = 1, J = 0) molecules [$C_6 = 1.533 \times 10^6$ atomic units (a.u.)] is essentially identical to that for (v = 0, J = 0) molecules ($C_6 = 1.525 \times 10^6$ a.u.) (*22*–*24*); thus, comparing collisions of Eqs. 1 and 2 should directly reveal the difference in their short-range physics. We find that, somewhat surprisingly, the losses have a very weak dependence on the chemical reactivity. Our result can be explained semiquantitatively by the model based on complex formation, but it also points out the importance of further understanding the properties and the post-formation dynamics of the complex.

RESULTS

Loss measurements with different chemical reactivities

The starting point of our experiment is an optically trapped sample of weakly bound NaRb Feshbach molecules (FMs) (*25*). To study and compare the collisions in Eqs. 1 and 2, we directly transfer the FMs to the target levels by a stimulated Raman adiabatic passage (STIRAP) (*11*).

Downloaded from http://advances.sciencemag.org/ on December 15, 2018

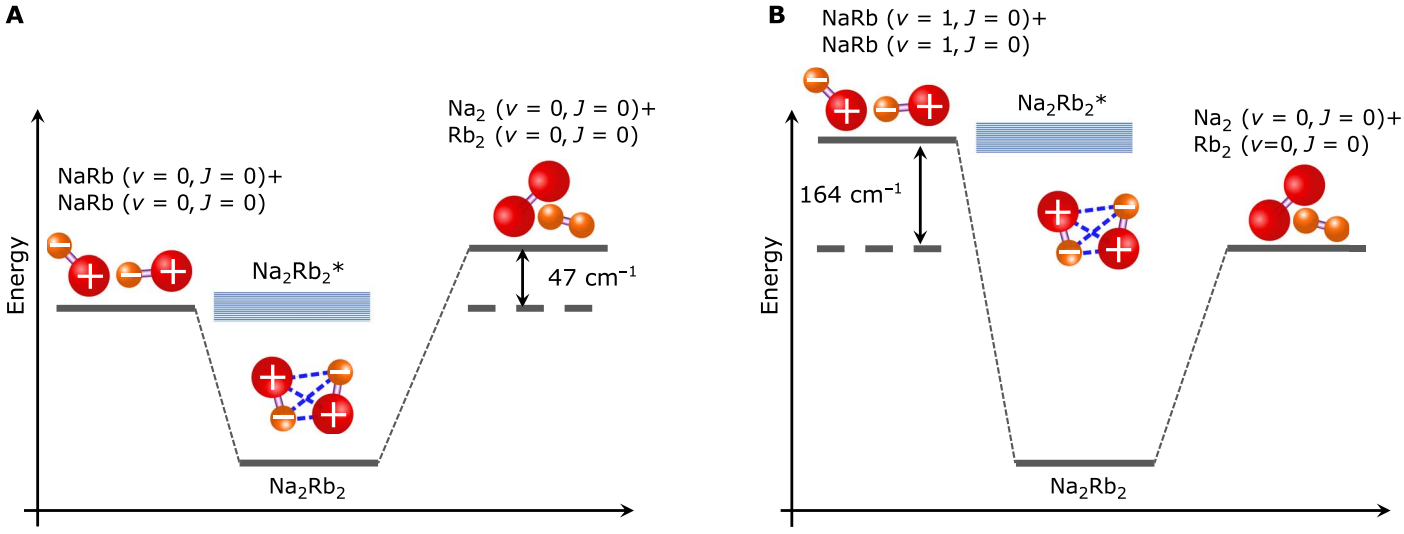

Fig. 1. Controlling the chemical reactivity of NaRb molecules by vibrational excitation. The schematic reaction coordinates for the NaRb + NaRb → Na_2 + Rb_2 process are shown. (**A**) In the lowest rovibrational level ($v = 0, J = 0$), the reaction is endothermic by 47 cm^{-1} and thus forbidden at ultracold temperatures. (**B**) In the first excited rovibrational level ($v = 1, J = 0$), the same reaction is already exothermic by 164 cm^{-1} and thus allowed. Molecules can also relax from $v = 1$ to $v = 0$ following the collision, but experimentally, this cannot be distinguished from chemical reactions. The ground Na_2Rb_2 tetramer level, which has much lower energy than both the reactant and product molecule pairs, is also shown. Near the NaRb + NaRb collision threshold, the density of Na_2Rb_2* states is estimated to be too large to be resolved. As a result, the collision is in the highly resonant regime (*12*).

With carefully chosen Raman laser frequency, power, and polarization combinations, we can create high-density samples of NaRb molecules in ($v = 0, J = 0$) and ($v = 1, J = 0$) with the nuclear hyperfine structures fully resolved (Fig. 2, A and B). We can also prepare molecules in the ($v = 0$, $J = 2$) level, which have even richer hyperfine Zeeman structures due to the nuclear spin-rotation coupling (Fig. 2C). However, investigating collisions with rotational relaxation is beyond the scope of this work.

Because we rely on absorption imaging of atoms for detection, a reversed STIRAP has to be applied to transfer the ground-state molecules back to the Feshbach state to be dissociated into atoms (*11*). By varying the delay time between the two STIRAP sequences, the evolution of the ground-state molecule number N can be measured. To increase detection sensitivity, we set up the imaging system along the long axis of the sample for higher integrated optical depths. This has allowed us to take long-duration measurements to cover a large range of molecule numbers. Figure 3A shows example measurements for both ($v = 0, J = 0$) and ($v = 1, J = 0$) molecules with initial number–to–final number ratios of nearly 40. Accompanying the fast losses, rapid temperature increases are also observed (Fig. 3B) because of the preferential removal of lower-energy molecules characteristic of all inelastic collisions (*26*, *27*).

A very striking feature in Fig. 3 is the number loss and the heating of the two cases being nearly identical, despite their distinctly different chemical reactivities and the very large range of number variations. To obtain a more quantitative picture, we simultaneously fit the number and temperature evolutions for each case to the two-body inelastic loss model (*26*)

$$\frac{dN(t)}{dt} = -\beta A \frac{N(t)^2}{T(t)^{3/2}}$$

$$\frac{dT(t)}{dt} = \beta A N(t) \frac{\frac{1}{4} + h_0}{T(t)^{1/2}} \quad (3)$$

to extract the loss rate constant β. Here, $A = (\bar{\omega} m / 4\pi k_B)^{3/2}$ is a constant, where m is the mass of the molecule and $\bar{\omega}$ is the geometric mean of the trap frequencies, which is measured to be $2\pi \times 119.9(1.5)$ Hz for ($v = 0$, $J = 0$) molecules and $2\pi \times 122.0(1.5)$ Hz for ($v = 1, J = 0$) molecules. The h_0 term deals with the momentum dependence of β as well as any other heating contributions. We note that the number loss and heating in Fig. 3 appear identical for the two cases, but because the trap frequencies are not the same, the β values are actually different.

Temperature dependence of loss rate constants

Initially, we used a constant β to fit the whole data set only to find that the values obtained vary with the initial sample temperatures. This indicates that β is changing during the course of the collisions following the temperature variation; thus, the collisions are not in the Wigner threshold region (*28*, *29*) in which $\beta \propto T^l$ should be a constant for S-wave ($l = 0$) collisions. This non-Wigner behavior can be understood by the much smaller characteristic temperature of the van der Waals potential $T_{vdW} = (\hbar^2 / m r_6^2)(1/k_B)$ for NaRb (*30*), which is only 2.8 μK because of the very large long-range C_6 coefficients (*22*–*24*). Here, $\hbar$ is Planck's constant h over 2π, k_B is Boltzmann's constant, and $r_6 = (mC_6/\hbar^2)^{1/4}$ is the characteristic length. The Wigner threshold region (*28*, *29*), which requires that $T << T_{vdW}$, is thus not reached with the current sample temperature.

To obtain β without knowing its exact T dependence, we have used the following procedure (*26*). We first divide a full measurement into several segments. During each segment, the temperature increases by less than 20%, and thus, β should change very little. We then fit each segment to Eq. 3, with the initial number, the initial temperature, the additional heating term h_0, and a constant β as free parameters. The same procedure is repeated for several data sets with initial temperatures ranging from 370 nK to 1.4 μK. Following the temperature increase, this has allowed us to sample β from 390 nK to 1.85 μK for the nonreactive molecules and from 500 nK to 1.85 μK for the reactive molecules. Figure 4 shows the results with the mean temperature of each corresponding

Downloaded from http://advances.sciencemag.org/ on December 15, 2018

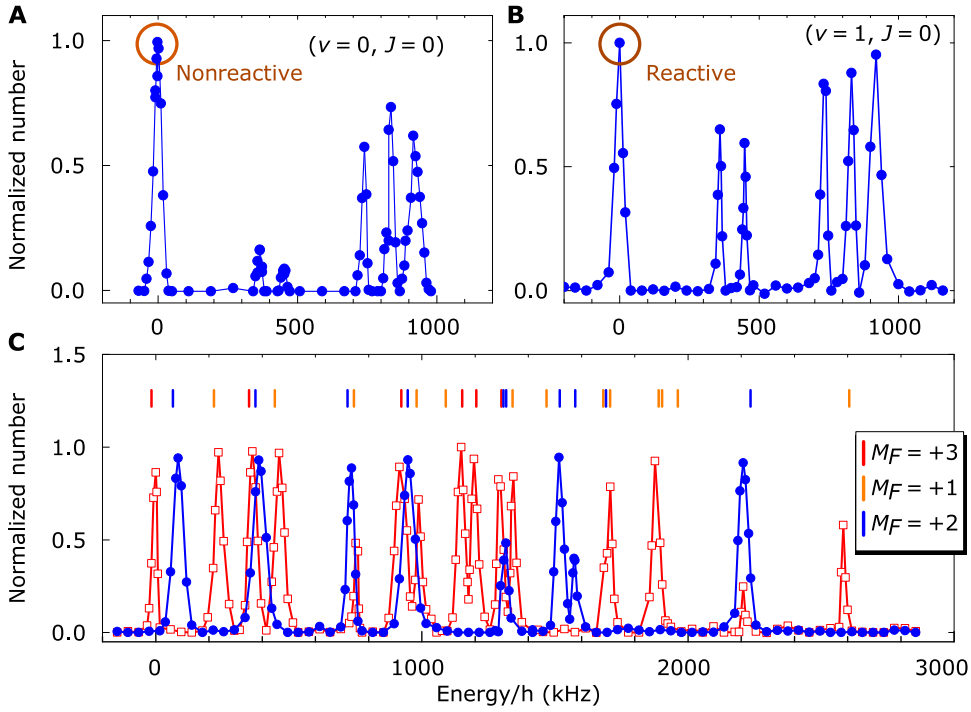

Fig. 2. High-resolution internal state control. (**A** to **C**) Well-resolved hyperfine structures of (A) the rovibrational ground state (v = 0, J = 0), (B) the first excited rovibrational state (v = 1, J = 0), and (C) the rotationally excited state (v = 0, J = 2). The two M_F = 3 hyperfine levels marked by the open circles in (A) and (B) are used in this work. (C) Spectra obtained with different Raman laser polarization combinations to demonstrate M_F control. The color-coded vertical bars in (C) mark the predicted hyperfine line positions.

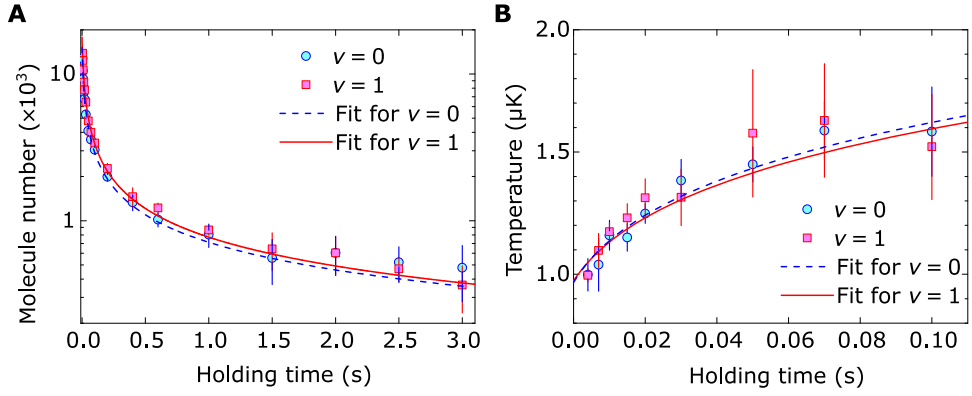

Fig. 3. Inelastic collisions with different chemical reactivities. (**A** and **B**) Time evolutions of (A) molecule numbers and (B) temperatures for both nonreactive (v = 0, J = 0) (filled circles) and reactive (v = 1, J = 0) (filled squares) samples. The temperature measurement, which stops at 0.1 s because of reduced signal-to-noise ratio following the time-of-flight expansion, is obtained separately from the number evolution with samples of essentially identical conditions. Error bars represent 1 SD. The blue dashed and red solid curves are fitting results using Eq. 3 with temperature-dependent loss rate constants obtained from Fig. 4 (see text for details). The measured trap oscillation frequencies are $[\omega_x, \omega_y, \omega_z] = 2\pi \times [217(3), 208(3), 38(2)]$ Hz for the (v = 0, J = 0) molecules and $2\pi \times [219(3), 205(2), 40(2)]$ Hz for the (v = 1, J = 0) molecules. The calculated initial peak densities can reach 6×10^{11} cm^{-3}.

segment as the horizontal axis. Within the temperature range covered, the lowest and the highest β values are only different by a factor of 2. This small dynamical range and the relatively large error bars prevented us from confirming any structures in β, although an overall decrease toward higher temperatures is obvious for both cases. In addition, the measured β values for nonreactive samples are all larger than those for the reactive ones within the same temperature range. In the log-log scale, forcing linear fits to the data points in Fig. 4, slopes of b = −0.38(4) and b = −0.27(8) can be obtained for nonreactive and reactive samples, respectively. Thus, approximately, during each set of measurements, the loss rate constant will follow a power-law function $\beta(T) = \beta_0 (T/T_0)^b$, where β_0 is the rate constant at a selected sample temperature T_0. After substituting β in Eq. 3 with this function and h_0 with $-b/6$, the number and temperature evolutions can be fitted again to obtain the β_0 values. For the data set of nonreactive molecules in Fig. 3, this kind of modeling gives $\beta_0 = 3.4(2) \times 10^{-10}$ cm^3 s^{-1} at $T_0 = 0.97(9)$ μK. For the

Downloaded from http://advances.sciencemag.org/ on December 15, 2018

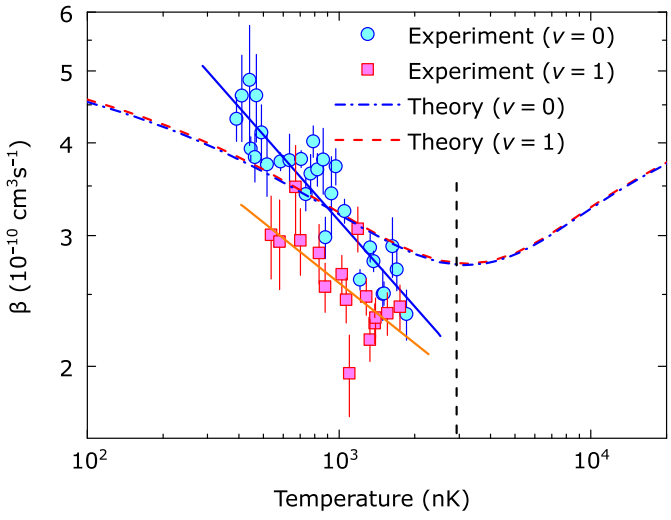

Fig. 4. Temperature dependence of β for different chemical reactivities. Each β is obtained from a fit to Eq. 3 to a segment of one full loss and heating measurement. The solid lines are from fits of β to power-law functions of *T*. Theoretical results based on the CC calculation are also shown. The dashed vertical line marks the position of T_{vdW}. The error bars represent 1 SD.

reactive molecules, $\beta_0 = 2.7(2) \times 10^{-10}$ cm^3 s^{-1} at $T_0 = 0.97(2)$ μK is obtained. Within the mutual error bars, the two β_0 values obtained this way agree with the corresponding data points around 0.97 μK in Fig. 4. This agreement verifies self-consistently that the β values obtained by the segment fitting method are reasonable.

Comparison with close-coupling quantum calculations

For the reactive case, the loss can be well understood with the universal model in which a unity reaction probability in the short range is used; thus, the rate constant and its temperature dependence are determined by the long-range collision dynamics (*3*, *30*–*33*). However, understanding the unexpected loss of the nonreactive molecules is more challenging. Thus far, the complex-mediated collision model is the only one attempting to explain it (*12*). For collisions (reactive or nonreactive alike) that proceed over a potential well, it is well known that a collision complex can be formed along the path (*1*). In the current experiment, because of the lack of convenient detection methods for the complex, its formation will manifest as loss of the NaRb molecules. To model this, following the conclusions from the highly resonant scattering picture for nonreactive molecules (*12*), we choose a full probability into the formation of the complex at the short range. In the study of Mayle *et al.* (*12*), it was shown that this is the same short-range boundary condition used in the universal model for reactive collisions; that is, complex formation has the same contribution to the loss as chemical reaction; thus, the loss rate constant from complex formation is also dictated by the long-range intermolecular interaction.

On the basis of this model, we performed close-coupling (CC) quantum calculations for both ($v = 0$, $J = 0$) and ($v = 1$, $J = 0$) NaRb molecules using a time-independent quantum formalism, including the rotational structure of the molecules and a partial wave expansion (*34*). As shown in Fig. 4, in terms of the absolute value of β, semiquantitative agreements between the calculations and the data can already be obtained without any free parameters. However, from the calculation, because the C_6 coefficient between two ($v = 0$, $J = 0$) NaRb molecules is nearly identical to that between two ($v = 1$, $J = 0$) NaRb molecules (*22*–*24*), the complex formation rate constant for nonreactive molecules (blue dashed-dotted curve) is essentially the same as the loss rate constant for reactive molecules (red dashed curve). This actually cannot explain the apparently larger β measured for nonreactive molecules. This discrepancy could reflect the idea that the short-range physics for chemical reaction and complex formation are not exactly identical. Although we have not attempted in the current work, it is possible to modify the rate constants for better agreements if more elaborate short-range models, including a non-unity reaction probability and the phase of the reflected scattering wave, were considered (*34*).

Possibility of post–complex formation dynamics

Another possible reason for the faster loss of ($v = 0$, $J = 0$) NaRb molecules is the complex-molecule collision, which is actually proposed as the main cause for the loss of nonreactive UPMs in the study of Mayle *et al.* (*12*) as a result of the long complex lifetime τ for nonreactive UPMs. In addition, the complex can also dissociate at a rate of $1/\tau$ to cause a revival of the original molecules. Intuitively, if the complex-molecule collision–induced loss is faster than the revival from complex dissociation, then it will cause additional loss of nonreactive molecules besides the complex formation and will result in a larger β following the two-body fit.

That the complex lifetime could be very long is a unique feature for nonreactive UPMs. This is attributed to the total angular momentum for a pair of colliding nonreactive ultracold absolute ground-state molecules, with both the internal rotation $J = 0$ and the external relative motion $l = 0$, being zero. Because of energy and angular momentum conservations, the number of open scattering channels for the complex, N_o, can only be one; in other words, the complex can only exit the potential well by dissociating back to the original molecules. On the other hand, near the collision threshold, using the same procedure as in the study of Mayle *et al.* (*12*), we estimated that the density of states ρ of the rotational and vibrational motion of the four-atom complex Na_2Rb_2* is on the order of 10^3/μK to 10^4/μK, which is very large. Thus, following the Rice-Ramsperger-Kassel-Marcus (RRKM) theory (*1*), the lifetime of the complex $\tau = 2\pi\hbar\rho/N_o$ could be 0.1 s to several seconds long. We emphasize that a long complex lifetime is only possible for nonreactive UPMs. For the chemical reactive case, τ should still be short even at ultracold temperatures owing to the large N_o from the many possible vibrational and rotational Na_2 and Rb_2 product levels. This short complex lifetime excludes both the complex-molecule collision and the complex revival; thus, the two-body model (Eq. 3) is enough to describe the reactive loss.

Confirming the complex-mediated collisions rigorously requires a detailed comparison between the experimental data and the full complex-mediated collision model. This model consists of two coupled rate equations: one for the molecule including losses from the complex formation and complex-molecule collision and the revival and the other for the complex including the complex formation and losses from both the complex-molecule collision and the complex dissociation (*12*). Unfortunately, because of the heating, the variation of β with temperature, and especially the unknown distribution of the complex and the possibly temperature-dependent complex-molecule rate constant, comparing our measurement to this model is very involved. Assuming that the complex and molecule always have the same temperature and that the complex has twice the polarizability of the molecule, but neglecting the temperature dependence of both rate constants, we constructed a

Downloaded from http://advances.sciencemag.org/ on December 15, 2018

model with the heating taken into account. The best fit of the nonreactive loss and heating data in Fig. 3 with this model results in a complex lifetime of $\tau = 0.038(6)$ s, which is shorter than the lower bound of our estimation from the RRKM theory, and a complex-molecule loss rate constant of $4.4(6) \times 10^{-9}$ cm^3 s^{-1}, which is more than one order of magnitude larger than the *S*-wave unitary limit and is thus nonphysical. Although this seems to support the absence of the complex-mediated collisions, we think that it is still not conclusive because of the crudeness of the approximations made in the model.

DISCUSSION

The ultimate way to solve all the aforementioned difficulties is by detecting the complex and studying the post–complex formation dynamics directly (*35*), for example, with the very sensitive state-resolved ionization detection method. Important information can also be learned by comparing the differences of collisions between two molecules and three molecules in the molecule assembly experiments with optical tweezers (*36*). In particular, with two molecules only, the complex-molecule collision is removed; thus, the complex lifetime can be directly measured by watching the time evolution of the molecule revival signal. This should allow a direct verification of the RRKM theory at the ultracold regime. Finally, besides its importance in ultracold chemistry, the existence of the complex should also be taken seriously in investigating dipolar many-body physics in optical lattices, for example, by considering multichannel Hubbard models (*37*).

MATERIALS AND METHODS

The optical trap potential was provided by a single-frequency high-power fiber laser operating at 1064.4 nm. This wavelength was far below all possible excited states for molecules in the lowest two vibrational levels of the $X^1\Sigma^+$ state and was also away from all resonances for FMs. The trap frequencies ω_x, ω_y, and ω_z of the ground-state molecules were obtained by measuring their center-of-mass oscillations in the optical potential. The measured values agree well with calculations based on theoretical polarizabilities at 1064.4 nm, which are 674.17 a.u. for ($v = 0$, $J = 0$) and 690.16 a.u. for ($v = 1$, $J = 0$) NaRb molecules (*38*).

The ($v = 1$, $J = 0$) level lies 3172.8 GHz above the rovibrational ground state. Owing to the fortuitously favorable transition strength, the same excited intermediate level for making ($v = 0$, $J = 0$) NaRb molecules with STIRAP described previously (*11*) can still be used here; thus, we only need to tune the dump laser frequency to create ($v = 1$, $J = 0$) molecules.

For the current investigation, it is crucial to prepare molecules in a single quantum state. Because of the atomic nuclear spins ($I_{Na} = I_{Rb} = {}^3/_2$), for the $J = 0$ states, there are 16 hyperfine Zeeman levels distributed in a small frequency span of ~1 MHz. As shown in Fig. 2 (A and B), these hyperfine structures, especially the lowest-energy ones for ($v = 0, J = 0$) and ($v = 1, J = 0$) with $M_F = 3$ used in this work (marked by open circles), can be fully resolved with carefully chosen Raman laser power and polarization combinations. Here, $M_F = m_I^{Na} + m_I^{Rb}$ is the projection of the total angular momentum, where m_I^{Na} and m_I^{Rb} are the projections of the Na and Rb nuclear spins, respectively. Experimentally, up to 1.5×10^4 NaRb molecules in either $M_F = 3$ hyperfine levels can be created routinely with STIRAP efficiencies around 93% and number fluctuations of typically less than ±5%. We have experimentally verified that the remaining population not in the ground state (about 7%) has negligible effects.

SUPPLEMENTARY MATERIALS

Supplementary material for this article is available at http://advances.sciencemag.org/cgi/content/full/4/1/eaaq0083/DC1

section S1. Extracting β with segment fit
section S2. Dependence of β on STIRAP efficiency
section S3. The complex-mediated collision model
fig. S1. Segment two-body fit for extracting the temperature dependence of β.
fig. S2. Dependence of β on STIRAP efficiency.
fig. S3. Checking the complex-mediated collisions.

REFERENCES AND NOTES

1. R. D. Levine, *Molecular Reaction Dynamics* (Cambridge Univ. Press, 2009).
2. R. V. Krems, Cold controlled chemistry. *Phys. Chem. Chem. Phys.* **10**, 4079–4092 (2008).
3. S. Ospelkaus, K.-K. Ni, D. Wang, M. H. G. de Miranda, B. Neyenhuis, G. Quéméner, P. S. Julienne, J. L. Bohn, D. S. Jin, J. Ye, Quantum-state controlled chemical reactions of ultracold potassium-rubidium molecules. *Science* **327**, 853–857 (2010).
4. T. Lahaye, C. Menotti, L. Santos, M. Lewenstein, T. Pfau, The physics of dipolar bosonic quantum gases. *Rep. Prog. Phys.* **72**, 126401 (2009).
5. M. A. Baranov, M. Dalmonte, G. Pupillo, P. Zoller, Condensed matter theory of dipolar quantum gases. *Chem. Rev.* **112**, 5012–5061 (2012).
6. D. DeMille, Quantum computation with trapped polar molecules. *Phys. Rev. Lett.* **88**, 067901 (2002).
7. A. André, D. DeMille, J. M. Doyle, M. D. Lukin, S. E. Maxwell, P. Rabl, R. J. Schoelkopf, P. Zoller, A coherent all-electrical interface between polar molecules and mesoscopic superconducting resonators. *Nat. Phys.* **2**, 636–642 (2006).
8. J. W. Park, S. A. Will, M. W. Zwierlein, Ultracold dipolar gas of fermionic $^{23}Na^{40}K$ molecules in their absolute ground state. *Phys. Rev. Lett.* **114**, 205302 (2015).
9. T. Takekoshi, L. Reichsöllner, A. Schindewolf, J. M. Hutson, C. R. Le Sueur, O. Dulieu, F. Ferlaino, R. Grimm, H.-C. Nägerl, Ultracold dense samples of dipolar RbCs molecules in the rovibrational and hyperfine ground state. *Phys. Rev. Lett.* **113**, 205301 (2014).
10. P. K. Molony, P. D. Gregory, Z. Ji, B. Lu, M. P. Köppinger, C. R. Le Sueur, C. L. Blackley, J. M. Hutson, S. L. Cornish, Creation of ultracold $^{87}Rb^{133}Cs$ molecules in the rovibrational ground state. *Phys. Rev. Lett.* **113**, 255301 (2014).
11. M. Guo, B. Zhu, B. Lu, X. Ye, F. Wang, R. Vexiau, N. Bouloufa-Maafa, G. Quéméner, O. Dulieu, D. Wang, Creation of an ultracold gas of ground-state dipolar $^{23}Na^{87}Rb$ molecules. *Phys. Rev. Lett.* **116**, 205303 (2016).
12. M. Mayle, G. Quéméner, B. P. Ruzic, J. L. Bohn, Scattering of ultracold molecules in the highly resonant regime. *Phys. Rev. A* **87**, 012709 (2013).
13. T. J. Odiorne, P. R. Brooks, J. V. V. Kasper, Molecular beam reaction of K with HCl: Effect of vibrational excitation of HCl. *J. Chem. Phys.* **55**, 1980–1982 (1971).
14. J. C. Polanyi, Concepts in reaction dynamics. *Acc. Chem. Res.* **5**, 161–168 (1972).
15. J. G. Pruett, R. N. Zare, State-to-state reaction rates: Ba+HF (v=0,1) → BaF (v=0–12)+H. *J. Chem. Phys.* **64**, 1774–1783 (1976).
16. R. N. Zare, Laser control of chemical reactions. *Science* **279**, 1875–1879 (1998).
17. P. S. Żuchowski, J. M. Hutson, Reactions of ultracold alkali-metal dimers. *Phys. Rev. A* **81**, 060703 (2010).
18. K. M. Jones, S. Maleki, S. Bize, P. D. Lett, C. J. Williams, H. Richling, H. Knöckel, E. Tiemann, H. Wang, P. L. Gould, W. C. Stwalley, Direct measurement of the ground-state dissociation energy of Na_2. *Phys. Rev. A* **54**, R1006 (1996).
19. J. Y. Seto, R. J. Le Roy, J. Vergès, C. Amiot, Direct potential fit analysis of the $X^1\Sigma_g^+$ state of Rb_2: Nothing else will do! *J. Chem. Phys.* **113**, 3067–3076 (2000).
20. A. Pashov, O. Docenko, M. Tamanis, R. Ferber, H. Knöckel, E. Tiemann, Potentials for modeling cold collisions between Na (3S) and Rb (5S) atoms. *Phys. Rev. A* **72**, 062505 (2005).
21. J. N. Byrd, J. A. Montgomery Jr., R. Côté, Structure and thermochemistry of K_2Rb, KRb_2, and K_2Rb_2. *Phys. Rev. A* **82**, 010502 (2010).
22. P. S. Żuchowski, M. Kosicki, M. Kodrycka, P. Soldán, van der Waals coefficients for systems with ultracold polar alkali-metal molecules. *Phys. Rev. A* **87**, 022706 (2013).
23. M. Lepers, R. Vexiau, M. Aymar, N. Bouloufa-Maafa, O. Dulieu, Long-range interactions between polar alkali-metal diatoms in external electric fields. *Phys. Rev. A* **88**, 032709 (2013).
24. R. Vexiau, M. Lepers, M. Aymar, N. Bouloufa-Maafa, O. Dulieu, Long-range interactions between polar bialkali ground-state molecules in arbitrary vibrational levels. *J. Chem. Phys.* **142**, 214303 (2015).
25. F. Wang, X. He, X. Li, B. Zhu, J. Chen, D. Wang, Formation of ultracold NaRb Feshbach molecules. *New J. Phys.* **17**, 035003 (2015).
26. J. Söding, D. Guéry-Odelin, P. Desbiolles, G. Ferrari, J. Dalibard, Giant spin relaxation of an ultracold cesium gas. *Phys. Rev. Lett.* **80**, 1869–1872 (1998).
27. T. Weber, J. Herbig, M. Mark, H.-C. Nägerl, R. Grimm, Three-body recombination at large scattering lengths in an ultracold atomic gas. *Phys. Rev. Lett.* **91**, 123201 (2003).

Downloaded from http://advances.sciencemag.org/ on December 15, 2018

28. H. A. Bethe, Theory of disintegration of nuclei by neutrons. *Phys. Rev.* **47**, 747–759 (1935).
29. E. P. Wigner, On the behavior of cross sections near thresholds. *Phys. Rev.* **73**, 1002–1009 (1948).
30. B. Gao, Universal model for exoergic bimolecular reactions and inelastic processes. *Phys. Rev. Lett.* **105**, 263203 (2010).
31. Z. Idziaszek, P. S. Julienne, Universal rate constants for reactive collisions of ultracold molecules. *Phys. Rev. Lett.* **104**, 113202 (2010).
32. G. Quéméner, J. L. Bohn, Strong dependence of ultracold chemical rates on electric dipole moments. *Phys. Rev. A* **81**, 022702 (2010).
33. K. Jachymski, M. Krych, P. S. Julienne, Z. Idziaszek, Quantum theory of reactive collisions for $1/r^n$ potentials. *Phys. Rev. Lett.* **110**, 213202 (2013).
34. G. Wang, G. Quéméner, Tuning ultracold collisions of excited rotational dipolar molecules. *New J. Phys.* **17**, 035015 (2015).
35. M. L. González-Martínez, O. Dulieu, P. Larrégaray, L. Bonnet, Statistical product distributions for ultracold reactions in external fields. *Phys. Rev. A* **90**, 052716 (2014).
36. L. R. Liu, J. T. Zhang, Y. Yu, N. R. Hutzler, Y. Liu, T. Rosenband, K.-K. Ni, Ultracold molecular assembly. arXiv:1701.03121 (2017).
37. A. Doçaj, M. L. Wall, R. Mukherjee, K. R. A. Hazzard, Ultracold nonreactive molecules in an optical lattice: Connecting chemistry to many-body physics. *Phys. Rev. Lett.* **116**, 135301 (2016).
38. R. Vexiau, D. Borsalino, M. Lepers, A. Orbán, M. Aymar, O. Dulieu, N. Bouloufa-Maafa, Dynamic dipole polarizabilities of heteronuclear alkali dimers: Optical response, trapping and control of ultracold molecules. *Int. Rev. Phys. Chem.* **36**, 709–750 (2017).

Acknowledgments: We are grateful to O. Dulieu and R. Vexiau for the valuable discussions and the polarizability calculation. **Funding:** This work was supported by the COPOMOL project, which was jointly funded by the Research Grants Council (RGC) of Hong Kong (grant no. A-CUHK403/13) and France's Agence Nationale de la Recherche (grant no. ANR-13-IS04-0004-01). The Hong Kong team was also supported by the National Basic Research Program of China (grant no. 2014CB921403) and the RGC General Research Fund (grant no. CUHK14301815). **Author contributions:** X.Y., M.G., and D.W. carried out the experiment and analyzed the data. M.L.G.-M. and G.Q. performed the CC calculation. X.Y. and D.W. wrote the manuscript with input from all authors. **Competing interests:** The authors declare that they have no competing interests. **Data and materials availability:** All data needed to evaluate the conclusions in the paper are present in the paper and/or the Supplementary Materials. Additional data related to this paper may be requested from D.W. (djwang@cuhk.edu.hk).

Submitted 20 September 2017
Accepted 28 December 2017
Published 26 January 2018
10.1126/sciadv.aaq0083

Citation: X. Ye, M. Guo, M. L. González-Martínez, G. Quéméner, D. Wang, Collisions of ultracold $^{23}Na^{87}Rb$ molecules with controlled chemical reactivities. *Sci. Adv.* **4**, eaaq0083 (2018).

Downloaded from http://advances.sciencemag.org/ on December 15, 2018

ScienceAdvances

Collisions of ultracold $^{23}Na^{87}Rb$ molecules with controlled chemical reactivities

Xin Ye, Mingyang Guo, Maykel L. González-Martínez, Goulven Quéméner and Dajun Wang

Sci Adv **4** (1), eaaq0083.
DOI: 10.1126/sciadv.aaq0083

ARTICLE TOOLS http://advances.sciencemag.org/content/4/1/eaaq0083

SUPPLEMENTARY MATERIALS http://advances.sciencemag.org/content/suppl/2018/01/22/4.1.eaaq0083.DC1

REFERENCES This article cites 36 articles, 2 of which you can access for free
http://advances.sciencemag.org/content/4/1/eaaq0083#BIBL

PERMISSIONS http://www.sciencemag.org/help/reprints-and-permissions

Use of this article is subject to the Terms of Service

Science Advances (ISSN 2375-2548) is published by the American Association for the Advancement of Science, 1200 New York Avenue NW, Washington, DC 20005. 2017 © The Authors, some rights reserved; exclusive licensee American Association for the Advancement of Science. No claim to original U.S. Government Works. The title *Science Advances* is a registered trademark of AAAS.

Downloaded from http://advances.sciencemag.org/ on December 15, 2018